

2021

Integration of Phase Change Material-Based Storage in Air Distribution Systems to Increase Building Power Flexibility

Philani Hlanze
University of Oklahoma, United States of America

Aly Elhefny

Zhimin Jiang

Jie Cai
University of Oklahoma, jcai@ou.edu

Hamidreza Shabgard

Follow this and additional works at: <https://docs.lib.purdue.edu/ihpbc>

Hlanze, Philani; Elhefny, Aly; Jiang, Zhimin; Cai, Jie; and Shabgard, Hamidreza, "Integration of Phase Change Material-Based Storage in Air Distribution Systems to Increase Building Power Flexibility" (2021). *International High Performance Buildings Conference*. Paper 366.
<https://docs.lib.purdue.edu/ihpbc/366>

This document has been made available through Purdue e-Pubs, a service of the Purdue University Libraries. Please contact epubs@purdue.edu for additional information. Complete proceedings may be acquired in print and on CD-ROM directly from the Ray W. Herrick Laboratories at <https://engineering.purdue.edu/Herrick/Events/orderlit.html>

Integration of Phase Change Material-Based Storage in Air Distribution Systems to Increase Building Power Flexibility

Philani HLANZE¹, Aly Elhefny¹, Zhimin JIANG¹, Jie CAI^{1*}, Hamidreza SHABGARD¹

¹School of Aerospace and Mechanical Engineering, University of Oklahoma
Norman, Oklahoma, 73019, USA

philanihlanze@ou.edu; jiangzhimin01@ou.edu; aly.elhefny@ou.edu; jcai@ou.edu; shabgard@ou.edu

* Corresponding Author

ABSTRACT

This paper presents a novel energy storage solution by incorporating phase change material (PCM) in the building supply-air duct to increase a building's thermal storage capacity. This solution has various advantages compared to PCM-integrated walls including more effective heat transfer (forced convection and greater temperature differentials). During off-peak hours, the system runs at a supply-air temperature below the material's solidification point to charge the PCM with cooling energy. During on-peak hours, a higher supply-air temperature is utilized so that the stored energy can be discharged into the supply-air. This shifts a portion of the building's cooling load from the on-peak hours to the off-peak hours. A numerical model for the melting and solidification of PCM in the duct was developed and modified using experimental data. Whole building energy simulations were conducted by coupling the PCM model with EnergyPlus DOE prototypical building model in a Simulink co-simulation platform. Simulations were performed for three cities in different climate zones over a three-month cooling season (June to August), and the PCM storage reduced the on-peak energy consumption by 20-25%. The electricity cost and payback period were determined using current time-of-use electricity rates.

1. INTRODUCTION

While the introduction of renewable energy sources has provided an alternative to fossil fuels with much reduced greenhouse gas emissions, their limited window of availability (particularly solar energy) has resulted in the rapid ramping of fossil fuel power plants to make up for the energy shortfall during the evening hours (Jones-Albertus, 2017). As a result, a lot of stress is put on these plants over a short period of time, which might shorten their lifespan and lower the overall generation efficiency. Thus, there is a need to shift the demand on the electricity grid to off-peak hours and create a more balanced daily supply and demand. In the US, commercial buildings and residential homes account for about 40% of the total energy consumption, and in commercial buildings, 32% of that energy is consumed by the Heating, Ventilation and Air-Conditioning (HVAC) systems (US Department of Energy, 2010). This makes commercial buildings an attractive area to implement energy savings and peak load reduction strategies. Thermal energy storage (TES) can be implemented in buildings using sensible heat or latent heat to alleviate the electrical power supply and demand imbalance issues on the electric grid (Iten *et al.*, 2016). Sensible heat storage involves using the building's thermal mass as a thermal battery by increasing or decreasing the temperature of the building envelope. Latent heat storage involves using a phase change material's (PCM) latent heat of fusion to store energy in the material during the phase change process.

The use of PCM as latent heat storage has previously been investigated in many studies. Iten *et al.* (2016) conducted a review of free cooling TES and PCM incorporated in the building envelope to increase the building's thermal mass. For PCM incorporated in the building envelope, the energy storage is driven by the increase or decrease in the outdoor or indoor temperatures, which initiates the melting or solidification process. Safari *et al.* (2016) investigated the implementation of PCM in roof and wall construction using the Fanger comfort model to control HVAC thermostat operation in Madrid's climate zone. They found that a PCM with 27 °C melting temperature resulted in the highest energy savings potential, and 5 mm thick modules resulted in a maximum of 16% annual energy savings and a minimum 6.38-year payback period for the office schedule. Neeper (2000) investigated the thermal dynamics of a wallboard impregnated with PCM. The study found that the maximum diurnal energy storage occurs at a value of the PCM melt temperature that is close to the average room temperature in most circumstances. The diurnal storage achieved in practice may be limited to a range of 300–400 kJ/m², even if the wallboard has a greater latent capacity.

Sleiti and Naimaster (2016) investigated the building energy performance of organic (fatty acid based) PCM products in ceiling constructions for a simulated quick service restaurant building model located in Atlanta, GA. PCM was added in the ceiling, in between the gypsum board and attic floor frame and insulation. The PCM cases considered were not able to achieve any changes in the zone air temperature that would translate to significant HVAC energy savings. One of the limitations for passive systems is that the air-to-PCM heat transfer is low due to the reliance on natural convection and the small temperature difference limits the effectiveness and heat penetration depth.

Free cooling TES has been previously investigated, and it involves using cold night-time air to cool the indoor space during the day. Takeda *et al.* (2004) investigated the reduction of the ventilation load during summer in various Japanese cities by installing a packed bed of PCM granules in the supply-air ventilation duct. When the outdoor air temperature is less than room air, two separate streams of outdoor air flow into the room and through the PCM bed to simultaneously charge the PCM and cool room. The air that leaves the PCM section is exhausted to the outdoor environment. When outdoor air temperature is higher than room air, outdoor air only passes through PCM bed and goes into room. The maximum ventilation load reduction was shown to be up to 62.8% in Kyoto; however, in the study the indoor air temperature was kept constant (26 °C) and heat transfer through the building walls was not considered. Yanbing *et al.* (2003) analyzed the thermal behavior of a Night Ventilation with PCM Packed Bed Storage (NVP) and determined convective heat transfer coefficients of 12 to 19 W/m²·°C and air flow resistance through the PCM of less than 20 Pa. Free cooling TES is attractive because it makes affective use of “free” energy source, but its main disadvantage is the requirement for bypass duct/dampers to allow for the active control of the charging/discharging periods and prevent overcooling of the indoor spaces.

The proposed PCM latent energy storage solution of the present study is displayed in Figure 1. The PCM is located in the supply-air duct in order to take advantage of the forced convection heat transfer provided by the moving air, which improves the rate of thermal penetration compared to PCM incorporated in the building envelope. The supply-air temperature (SAT) will be lowered to initiate the PCM solidification (PCM charging) and store “cooling” energy in the PCM. When needed, the SAT is increased to initiate the PCM melting process (PCM discharging). The PCM charging process is conducted during the off-peak hours and the PCM discharging process is enabled during on-peak hours to reduce electrical energy usage and peak demand. This increases the HVAC cooling load during the PCM charging and decreases it during the PCM discharging. When implemented with time-of-use (TOU) electricity rates, the building electricity cost can be effectively reduced. The solution does not require any bypass duct or dampers, so it is easier to retrofit than most of the free cooling solutions.

The objective of this paper is to evaluate the energy cost savings and peak electric demand reduction that can be achieved by installing PCM in the supply air duct of the HVAC system. This objective will be achieved by formulating a model for the melting and solidification of PCM in the duct, conducting a whole building simulation for a PCM-equipped medium office building in different climate zones using an EnergyPlus-Simulink co-simulation platform, and calculating the energy cost savings and payback period using current TOU rates.

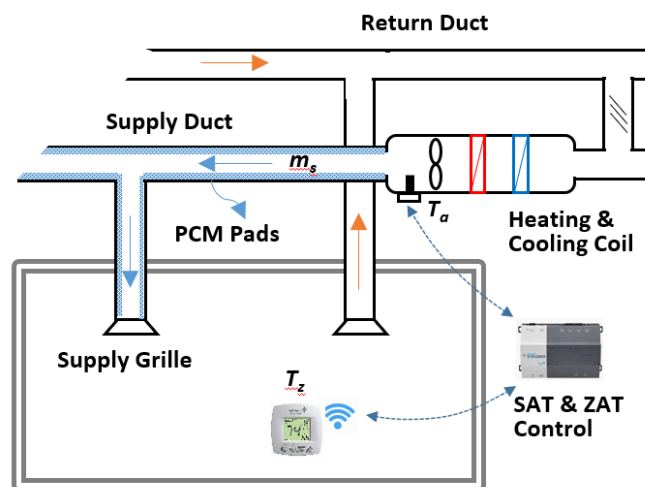


Figure 1: Proposed PCM storage location

2. WHOLE BUILDING SIMULATION

2.1 PCM Model

The PCM is mounted on the interior surfaces of the vertical and horizontal supply duct walls. Heat is transferred between the air and PCM through the PCM casing. The duct wall is assumed to be well insulated with external insulation and no heat is lost through the duct wall. The PCM model used in the whole building simulation is adapted from the Enthalpy method (Faghri & Zhang, 2006). The heat transfer in the PCM is modeled as a one-dimensional conduction-controlled, two-region melting problem in a finite slab. The density of the solid and liquid phases is assumed to be equal ($\rho_s = \rho_l = \rho$), and the governing equation is

$$\rho \frac{\partial h}{\partial t} = \frac{\partial}{\partial x} \left(k \frac{\partial T}{\partial x} \right) \quad (1)$$

where h is the PCM enthalpy, t is time, x is distance, k is the PCM thermal conductivity and T is temperature. The enthalpy is defined as

$$h(T) = \begin{cases} c_{ps}(T - T_m) & T < T_m \\ 0 & T = T_m, \text{ fully solidified} \\ h_{sl} & T = T_m, \text{ fully melted} \\ c_{pl}(T - T_m) + h_{sl} & T > T_m \end{cases} \quad (2)$$

where h_{sl} is the PCM latent heat, T_m is the PCM melting temperature, and c_{pl} and c_{ps} are the liquid and solid PCM specific heat, respectively. In simulations, the PCM is initially either fully solid or liquid, but during melting/solidification, h is between 0 and h_{sl} . The PCM thermal conductivity is assigned according to the phase:

$$k(T) = \begin{cases} k_s & T \leq T_m, \quad h(T) \leq 0 \\ k_l & T \geq T_m, \quad h(T) \geq h_{sl} \end{cases} \quad (3)$$

where k_s and k_l are the solid and liquid thermal conductivities, respectively. Equation (1) is discretized using a forward difference in time and central difference in space, and the enthalpy at the $(n+1)^{\text{th}}$ timestep is determined as follows:

$$h_j^{n+1} = \frac{\Delta t}{\rho(\Delta x_{PCM})^2} (k_{j+\frac{1}{2}} T_{j+1}^n + k_{j-\frac{1}{2}} T_{j-1}^n) + \left(h_j^n - \frac{\Delta t (k_{j+\frac{1}{2}} + k_{j-\frac{1}{2}})}{\rho(\Delta x_{PCM})^2} T_j^n \right) \quad (4)$$

where Δt is the timestep, Δx_{PCM} is the PCM nodal thickness, and the location and time are represented by j and n , respectively. Figure 2 displays how the nodes in the PCM are arranged. The thermal conductivities at the half-grid, $k_{j+\frac{1}{2}}$ and $k_{j-\frac{1}{2}}$, are calculated using the harmonic mean method:

$$k_{j+\frac{1}{2}} = \frac{2k_j k_{j+1}}{k_j + k_{j+1}} \quad (5)$$

$$k_{j-\frac{1}{2}} = \frac{2k_j k_{j-1}}{k_j + k_{j-1}} \quad (6)$$

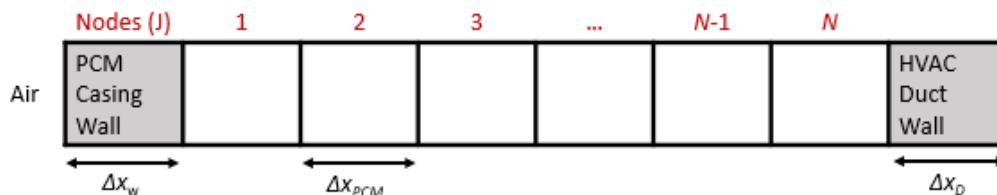


Figure 2: PCM model node arrangement

The enthalpy at node N , which is adjacent to the duct wall, is calculated using

$$h_N^{n+1} = \frac{\Delta t}{\rho(\Delta x_{PCM})} \left(\frac{k_{N-\frac{1}{2}}(T_{N-1}^n - T_N^n)}{\Delta x_{PCM}} - \frac{T_N^n - T_D^n}{\frac{\Delta x_D/2}{k_D} + \frac{\Delta x_{PCM}/2}{k_N}} \right) + h_N^n \quad (7)$$

where T_D is the duct temperature, Δx_D is the duct wall thickness, and k_D is the duct thermal conductivity. Once the enthalpy at each node is determined, the temperature is found using

$$T_j^{n+1} = \begin{cases} T_m + \frac{h_j^{n+1}}{c_{ps}} & h_j^{n+1} \leq 0 \text{ (solid)} \\ T_m & 0 < h_j^{n+1} < h_{sl} \text{ (interface)} \\ T_m + \frac{h_j^{n+1} - h_{sl}}{c_{pl}} & h_j^{n+1} \geq h_{sl} \text{ (liquid)} \end{cases} \quad (8)$$

The heat transfer into the duct wall is calculated as

$$m_D c_D \frac{T_D^{n+1} - T_D^n}{\Delta t} = \frac{T_N^n - T_D^n}{\frac{\Delta x_D/2}{k_D A} + \frac{\Delta x_{PCM}/2}{k_{PCM} A}} \quad (9)$$

where m_D is the duct wall node mass, c_D is the duct wall specific heat, and A is the area perpendicular to the heat flow.

The air-to-PCM heat transfer was modeled using the convection correlations for internal turbulent flow, specifically the *Dittus-Boelter correlation* (Bergman *et al.*, 2011). The convective heat transfer coefficient (U) is calculated as

$$U = 0.023 Re_D^{4/5} Pr^b \frac{k_a}{D_h} \quad (10)$$

where Re_D is the Reynolds number, Pr is the Prandtl number, k_a is the thermal conductivity of the air, D_h is the hydraulic diameter, and b is 0.4 for PCM cooling and 0.3 for PCM heating. The Prandtl number is calculated using

$$Pr = \frac{c_{pa} \mu}{k_a} \quad (11)$$

where c_{pa} is the specific heat of the air, and μ is the dynamic viscosity. The Reynolds number is calculated using

$$Re_D = \frac{\rho_a v D_h}{\mu} \quad (12)$$

where ρ_a is the air density, v is the air velocity. The hydraulic diameter is calculated using

$$D_h = \frac{4A_c}{P} \quad (13)$$

where A_c is the duct cross-sectional area and P is the wetted perimeter. The heat transfer through the PCM casing wall is calculated using

$$m_w c_w \frac{T_w^{n+1} - T_w^n}{\Delta t} = \frac{T_{air}^n - T_w^n}{\frac{1}{UA} + \frac{\Delta x_w/2}{k_w A}} - \frac{T_w^n - T_1^n}{\frac{\Delta x_w/2}{k_w A} + \frac{\Delta x_{PCM}/2}{k_{PCM} A}} \quad (14)$$

where m_w is the mass of the PCM casing wall, c_w is the specific heat of the PCM casing wall, T_w is the temperature of the PCM casing wall, T_{air} is the air temperature, Δx_w is the wall thickness, k_w is the wall thermal conductivity and T_1 is the temperature of the PCM node adjacent to the wall. The enthalpy of the first PCM node is calculated using

$$h_1^{n+1} = \frac{\Delta t}{\rho(\Delta x_{PCM})} \left(\frac{q_{out}}{A} - \frac{k_{1+\frac{1}{2}}(T_1^n - T_2^n)}{\Delta x_{PCM}} \right) + h_1^n \quad (15)$$

where

$$q_{out} = \frac{T_w^n - T_1^n}{\frac{\Delta x_w/2}{k_w A} + \frac{\Delta x_{PCM}/2}{k_{PCM} A}} \quad (16)$$

The length of the duct is divided into different sub-sections and the PCM model is evaluated at each sub-section in a sequence from the inlet to the outlet sub-section. The outlet air of the previous subsection is considered the inlet air of the next section. The temperature of the air entering the next duct sub-section is calculated using

$$T_{out} = T_{in} - \frac{q_{in}}{\dot{m}_a c_{pa}} \quad (17)$$

where \dot{m}_a is the air mass flow rate and

$$q_{in} = \frac{T_{air}^n - T_w^n}{\frac{1}{UA} + \frac{\Delta x_w / 2}{k_w A}} \quad (18)$$

2.2 PCM Model Modification

We performed a small-scale experiment to determine possible heat transfer enhancement of adding fins to the PCM module. The test was conducted by placing a 1" deep acrylic tray that is filled with PCM and covered by a finned aluminum sheet downstream of an Air Handling Unit (AHU). Thermocouples were placed in the tray at 0.25" depth intervals. The PCM used in the experiment was PureTemp 15, which is a biobased PCM with a nominal melting point of 15 °C (PureTemp, 2020). The experiment was conducted in two stages: the first stage consisted of solidifying the PCM that was initially in the liquid phase, and the second stage consisted of melting the PCM directly after the first stage. During the first stage, the supply-air temperature was set at 9 °C, and the airflow rate was set to 700 CFM. During the second stage, the supply-air temperature was set to 19 °C, and the airflow rate was set to 1475 CFM to achieve a similar cooling rate to the first stage. The experimental data was used to estimate a heat transfer enhancement factor to the PCM model associated with the addition of fins. The three parameters chosen to apply the enhancement factor are the air-side convective heat transfer coefficient and the solid and liquid PCM thermal conductivities, since the addition of fins enhances both the air-to-PCM convection and in-PCM conduction heat transfer. The factor was applied using a scalar multiplier, z , where

$$\begin{aligned} h_{air,enhanced} &= h_{air} * z \\ k_{s,enhanced} &= k_s * z \\ k_{l,enhanced} &= k_l * z \end{aligned} \quad (19)$$

The enhancement factor z was estimated to be 8.5 using a nonlinear curve fitting.

2.3 EnergyPlus and Simulink Co-simulation Platform

The whole building energy simulation was performed using an EnergyPlus co-simulation platform in Simulink that was developed by the team. The EnergyPlus Functional Mock-up Unit (FMU) file contains the building energy models and is linked to the PCM model using three primary interfacing variables, which are updated at each timestep in a ping-pong scheme. The EnergyPlus FMU outputs the supply-air mass flow rate and supply air temperature, which are inputs to the PCM model. The PCM model outputs the PCM section's outlet air temperature. The EnergyPlus FMU then inputs this temperature as the air temperature being supplied to the individual zones. The building type used in the co-simulation was the three-floor prototypical medium office building, which contains 15 conditioned zones (3 core zones and 12 perimeter zones). Each floor has a dedicated AHU and a direct-expansion air-conditioning system. Each zone has a variable air volume terminal with reheat. The whole building simulation was conducted for multiple cities to understand how the performance of the proposed PCM storage is affected by the climate location. The candidate cities were Miami, Florida (1A), El Paso, Texas (3B) and Buffalo, New York (5A).

The whole building simulations consist of two cases: baseline and PCM-equipped. The baseline case simulates normal HVAC operation without the PCM in the duct and the SAT setpoint is set at a constant value of 12.7 °C. In this case, there is no interaction between the EnergyPlus FMU and the PCM model. The PCM-equipped case involves lowering the SAT setpoint to 9.2 °C from 6 AM to 12 PM (PCM charging period) and raising the SAT setpoint to 15.2 °C from 12 PM to 3 PM and 15.7 °C from 3 PM to 6 PM. The period from 12 PM to 6 PM (PCM discharging period) corresponds with the on-peak energy hours. For the rest of the day, the SAT setpoint assumes 12.7 °C when mechanical cooling is requested. The simulations were conducted for a 3-month cooling season from the beginning of June to the end of August. For each case, the timestep in the EnergyPlus simulation is ten minutes. To ensure that convergence requirements for the Enthalpy method are met, the timestep in the PCM model is 0.5 s, which is implemented inside the MATLAB function block in Simulink.

2.4 PCM and Duct Sizing

The PCM mass was sized for each floor of the medium office building according to the on-peak HVAC sensible cooling energy usage for the hottest day of the whole cooling season. The baseline case was simulated for the 3-month

cooling season and the day with the highest on-peak total HVAC sensible cooling energy (Q_s) was used as the design day. The PCM was sized to have total latent heat energy equal to one tenth of the on-peak HVAC sensible cooling energy use of the design day:

$$m_{PCM} = \frac{Q_{s,max\ on-peak}}{10 h_{sl}} \quad (20)$$

The duct in each floor was sized according to the maximum design airflow rate (\dot{V}_{max}) determined by EnergyPlus. The square duct width (W_d) was determined as

$$W_d = \sqrt{\frac{\dot{V}_{max}}{v_{max}}} \quad (21)$$

where v_{max} is the maximum recommended air velocity in a duct (1200 fpm). The duct wall thickness is set at 1.31 mm, which corresponds with 16-gauge galvanized steel. The total length of the PCM duct section was 20 m and it was divided into 20 lengthwise subsections. The PCM thickness was determined using the PCM mass, total duct length and duct width.

3. SIMULATION RESULTS AND DISCUSSION

This section presents the results of the whole building simulation and the analysis to deduce meaningful insights on the load shifting capabilities of the PCM thermal energy storage. First, one day results for hot-dry and mild-humid days are presented and analyzed for El Paso. These two days were chosen because they have weather conditions that have high sensible and latent cooling loads, which will give insight into how these loads are shifted and their effect on the peak energy demand reduction. Then, the 3-month cooling season loads and energy costs are presented for each location. Lastly, the payback period for each location is determined.

3.1 El Paso Representative Day Results

Figures 3A and 3B display the total HVAC cooling load profiles for the baseline and PCM-equipped cases on hot-dry and mild-humid days. The total cooling load shifted from the on-peak to the off-peak hours on the hot-dry day is 414 MJ, which is 12.0 % of the baseline on-peak total cooling load. The total cooling load shifted from the on-peak to the off-peak hours on the mild-humid day is 586 MJ, which is 21.3 % of the baseline on-peak total cooling load. The shift in the total cooling load is caused by the shift in the sensible and latent cooling loads. The addition of the PCM results in an increase in the HVAC sensible load during the charging period due to the lower supply-air temperature and a decrease in the HVAC sensible load during the discharging period due to the higher supply-air temperature. The sensible cooling load that is shifted from the on-peak hours to the off-peak hours on the hot-dry day is 389 MJ, which equates to 11.4 % of the baseline on-peak sensible load. The sensible load that is shifted from the on-peak hours to the off-peak hours on the mild-humid day is 306 MJ, which equates to 14.9 % of the baseline on-peak sensible load. The addition of the PCM also results in an increase in the HVAC latent cooling load during the charging period and a decrease during the discharging period. The load is higher during the charging period in the PCM-equipped case because the supply air temperature is lower, which leads to a lower evaporating temperature and more removal of water vapor from the air. Conversely, the supply air temperature is higher in the discharging period, which results in less dehumidification because of the higher evaporating temperature and lower moisture level in the re-circulating air. The amount of the latent load that is shifted from the on-peak hours to the off-peak hours on the hot-dry day is 25.7 MJ, which equates to 52.9 % of the baseline on-peak latent load. The amount of the latent load that is shifted from the on-peak hours to the off-peak hours on the mild-humid day is 279 MJ, which equates to 40.2% of the baseline on-peak latent load. The mild-humid day has a higher latent cooling load than the hot-dry day due to the higher moisture content of the air in the outdoor environment.

Figure 3C displays the total HVAC electric power consumption profile for the baseline and PCM-equipped cases on hot-dry and mild-humid days. The amount of the electric power that is shifted from the on-peak hours to the off-peak hours on the hot-dry day is 47.9 kWh, which equates to 17.6 % of the baseline on-peak electric load. The on-peak peak demand of the HVAC electric power on the hot-dry day was reduced by 9.65 kW, which equates to a reduction by 17.8 %. The amount of the electric load that is shifted from the on-peak hours to the off-peak hours on the mild-humid day is 31.9 kWh, which equates to 25.3 % of the baseline on-peak total electric load. The on-peak peak demand of the HVAC electric power on the mild-humid day was reduced by 6.63 kW, which equates to a reduction by 24.0 %. The total HVAC electric power consists of the compressor power and supply air fan power. In the PCM case, the

compressor power consumption is partially shifted from the on-peak to the off-peak period because less power input is needed to provide the lower amount of cooling required. However, there is an increase in the supply fan power consumption in the on-peak period because the higher SAT results in a high supply airflow rate to provide sufficient indoor cooling. Although the fan power is increased during the on-peak hours, the compressor power reduction is dominant leading to much reduced on-peak HVAC electricity usage.

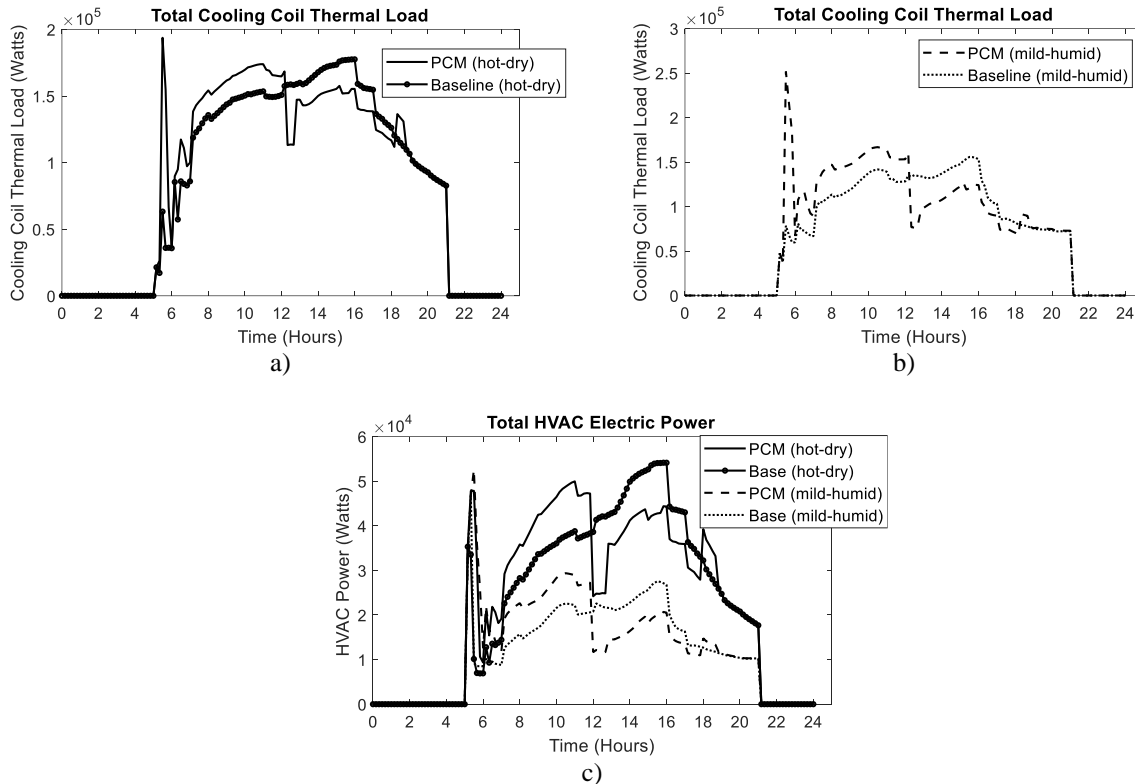


Figure 3: HVAC cooling load and electric consumption profiles for hot-dry and mild-humid days in EL Paso

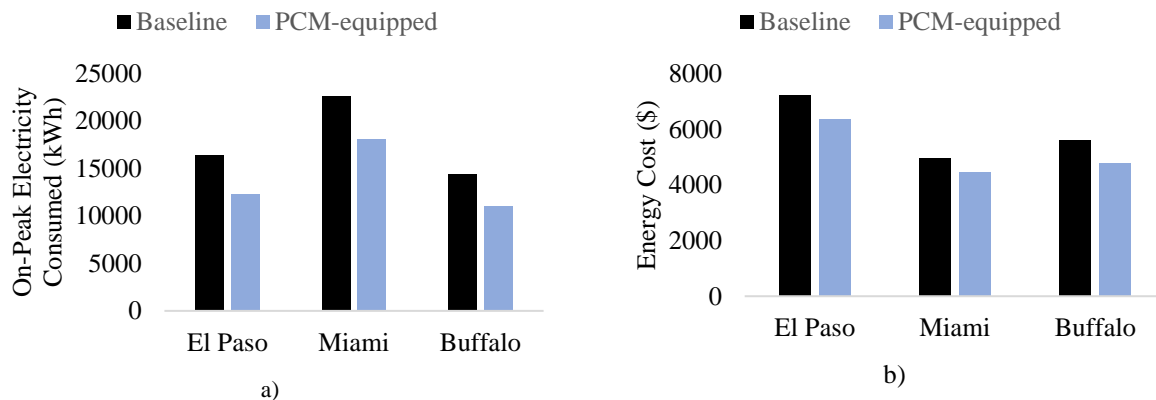
3.2 Total HVAC Energy Consumption and Cost

The total HVAC energy cost was calculated using the summer TOU electricity rates charged by energy providers in the three locations. Table 1 displays a breakdown of the utility tariffs used in the simulations. The rates comprise two charges: the energy charge and the demand charge. The energy charge is the cost of the electrical energy (\$/kWh) and is calculated at each timestep according to the specific rate at that time. The demand charge is the cost of providing the highest electrical demand, in kW, over a 30-minute interval in a month and is calculated at the end of each month.

The total on-peak HVAC electricity consumption and HVAC electricity cost are displayed in Figure 4 for the baseline and PCM-equipped cases in El Paso, Miami and Buffalo over the duration of the 3-month cooling season. The total on-peak electric consumption was reduced by 4074 kWh (25.0%) in El Paso, 4511 kWh (20.0%) in Miami and 3349 kWh (23.4%) in Buffalo. Miami had the highest on-peak electricity consumption due to the hot and humid climate, which leads to high sensible and latent cooling loads. As a result, there was a higher amount of load shifting that took place. The total electricity cost was reduced by \$889.00 (12.3%) in El Paso, \$472.00 (9.6%) in Miami and \$812.00 (14.5%) in Buffalo. Despite having the highest total decrease in on-peak electricity consumption, Miami had the lowest electricity cost saving because it had the least aggressive rate variation. The on-peak energy charge is 24x higher in El Paso, 2x higher in Miami and 16x higher in Buffalo than the off-peak charge. Therefore, the rate schedule in Miami does not incentivize load shifting as much compared to El Paso and Buffalo.

Table 1: Summer energy and demand rates for the three locations

City	Rate name	Energy rate (\$/kWh)			Demand Charge (\$/kW)	
		On-Peak	Mid-peak	Off-peak	On-peak	Anytime
El Paso	EL PASO ELECTRIC COMPANY SCHEDULE NO. 24 (El Paso Electric Company, 2017)	0.11861 (12-6PM)	—	0.00502 (12AM-12PM and 6PM-12AM)	—	24.50
Miami	Florida Power & Light Company General Service Demand-TOU (GSDT-1) (Florida Power & Light Company, 2020)	0.07078 (12-9PM)	—	0.03272 (12AM-12PM and 9PM-12AM)	9.98	—
Buffalo	Orange and Rockland Utilities Time of Use (Orange and Rockland Utilities Inc, 2020)	0.32012 (12-7PM)	0.1145 (10AM-12PM and 7-9PM)	0.02061 (12AM-10AM and 9PM-12AM)	—	—

**Figure 4:** Total on-peak electricity consumed by HVAC system and energy cost for the baseline and PCM-equipped cases in various cities

3.3 Cooling Season Energy and Cost Summary

Table 2 displays the total loads, electric energy and electricity cost for the whole simulation period in El Paso, Miami and Buffalo, respectively. Miami had the highest total cooling load due to high sensible and latent load, which is characteristic of the hot-humid climate. This climate has the highest potential for load shifting because the implementation of the PCM TES will shift both the sensible and the latent load. For all cities, the average system COP is slightly lower in the PCM-equipped case than the baseline case. This is because the increase in the COP during the PCM discharging period is smaller than the decrease during the PCM charging period. Despite using more electric energy overall, the electricity cost is lower in all cities because the consumption was shifted from the on-peak hours to the off-hours, leveraging the use of cheaper electricity during off-peak hours.

Table 2: El Paso - Cooling season total energy and electricity cost

	El Paso		Miami		Buffalo	
	Baseline	PCM-equipped	Baseline	PCM-equipped	Baseline	PCM-equipped
Cooling Coil Total Load (GJ)	607	643	880	924	639	672
Total Electric Energy (MWh)	38.7	41.5	54.3	58.8	34.3	37.2
System COP	4.4	4.3	4.5	4.4	5.2	5.0
Total PCM (kg)	—	1915	—	2418	—	1902
Total Electricity Cost (\$)	7227	6338	4940	4468	5582	4770
On-Peak Electric Energy (kWh)	16325	12251	22602	18091	14332	10983

3.4 Payback Analysis

A simple payback analysis was performed to determine how long it would take to recover the cost of the PCM. The payback years were calculated as follows:

$$\text{Payback years} = \frac{\text{Cost of PCM}}{\text{Annual Cooling Season Electricity Cost}} \quad (22)$$

The cost of the PCM was assumed to be \$2 per kg (Kosny *et al.*, 2013). The payback years for each city are displayed in Table 3. El Paso had the lowest payback period (4.3 years) among the cities. This was due to the high energy cost savings in El Paso and a relatively low total PCM cost. Buffalo had a slightly higher payback period (4.7 years) because it had lower energy cost savings and similar PCM cost. Since Miami used the most PCM and involved the lowest energy cost saving, it had the longest payback period (10.2 years).

Table 3: Payback years for PCM cost in the candidate cities

City	PCM Cost (\$)	Payback years
El Paso	3830	4.3
Miami	4836	10.2
Buffalo	3804	4.7

4. CONCLUSION

In this paper, the energy cost savings, on-peak load shifting, and peak electric demand reduction potentials were evaluated for a PCM-based TES system designed for installations in supply-air duct. A numerical model for the PCM in the duct was formulated and calibrated using experimental data. The model was linked with EnergyPlus through FMU to perform whole building simulations for a medium office in three different climate regions over a 3-month cooling season. The PCM TES was able to shift the sensible HVAC load from the on-peak to off-peak hours due to the lowering of the SAT to store “cooling” energy in the PCM during the charging process and raising of the SAT to release the “cooling” energy in the PCM during the discharging process. Due to the lower SAT during the charging process, there was more dehumidification in the morning. On the other hand, there was less dehumidification during the afternoon hours when the SAT was raised. This led to a shift in the latent HVAC load from the on-peak to off-peak hours. The shift in the total cooling load resulted in a shift in the HVAC electric power consumption because less work input is required to provide cooling within the on-peak hours and more work input is required to provide the additional cooling in the off-peak hours. Miami had the highest on-peak load reduction because its hot-humid climate meant that it had a high sensible load, which led to a large PCM size, and high latent load. However, since it had the least aggressive price difference between on-peak and off-peak hours, it had the lowest electricity cost savings. El Paso had the most aggressive TOU rate schedule, so it had the highest energy cost savings. Similarly, El Paso had the shortest payback period of 4.3 years. In actual building operations, the payback period is expected to be shorter when the cost analysis is extended to other months where space cooling is still required; for commercial buildings whose cooling loads are mainly internal gain driven, space cooling is usually required throughout the whole year.

REFERENCES

- Bergman, T. L., Lavine, A. S., Incropera, F. P., & Dewitt, D. P. (2011). *Fundamentals of Heat and Mass Transfer* (7th ed.). Hoboken: Wiley.
- El Paso Electric Company. (2017, July 18). *Schedule No. 24 General Service Rate*.
https://www.epelectric.com/files/html/Rates_and_Regulatory/13_-_Rate_24_General_Service_Rate.pdf
- Faghri, A., & Zhang, Y. (2006). *Transport Phenomena in Multiphase Systems*. Amsterdam: Elsevier.
- Florida Power & Light Company. (2020, June). *Business rates and clauses*.
[https://www.fpl.com/content/dam/fpl/us/en/rates/pdf/Business%20\(Effective%20June%202020\).pdf](https://www.fpl.com/content/dam/fpl/us/en/rates/pdf/Business%20(Effective%20June%202020).pdf)
- Iten, M., Liu, S., & Shukla, A. (2016). A review on the air-PCM-TES application for free cooling and heating in the buildings. *Renewable and Sustainable Energy Reviews*, 61, 175-186.
- Jones-Albertus, B. (2017, October 12). *Confronting the Duck Curve: How to Address Over-Generation of Solar Energy*. (Office of Energy Efficiency and Renewable Energy)
<https://www.energy.gov/eere/articles/confronting-duck-curve-how-address-over-generation-solar-energy>
- Kosny, J., Shukla, N., & Fallahi, A. (2013). *Cost Analysis of Simple Phase Change Material-Enhanced Building Envelopes in Southern U.S. Climates*. US Department of Energy.
- Neeper, D. (2000). Thermal dynamics of wallboard with latent heat storage. *Solar Energy*, 68(5), 393-403.
- Orange and Rockland Utilities Inc. (2020). *Time-of-Use Rates*. <https://www.oru.com/en/save-money/energy-saving-programs/time-of-use>
- PureTemp. (2020). *PureTemp 15 Technical Data Sheet*. <http://www.puretemp.com/stories/puretemp-15-tds>
- Saffari, M., de Gracia, A., Ushak, S., & Cabeza, L. (2016). Economic impact of integrating PCM as passive system in buildings using Fanger comfort model. *Energy and Buildings*, 112, 159-172.
- Sleiti, A. K., & Naimaster, E. J. (2016). Application of Fatty Acid Based Phase-Change Material to Reduce Energy Consumption From Roofs of Buildings. *Journal of Solar Energy Engineering*, 138(5), 051003.
- Takeda, S., Nagano, K., Mochida, T., & Shimakura, K. (2004). Development of a ventilation system for granules containing phase change material. *Solar Energy*, 77, 329-338.
- US Department of Energy. (2010). *Energy Efficiency Trends in Residential and Commercial Buildings*.
https://www1.eere.energy.gov/buildings/publications/pdfs/corporate/building_trends_2010.pdf
- Yanbing, K., Yi, J., & Yinping, Z. (2003). Modeling and experimental study on an innovative passive cooling system—NVP system. *Energy and Buildings*, 35(4), 417-425.